ZnO as effective luminescent sensing materials for nitroaromatic derivatives

Roy Aad, Vesna Simic, Loïc Le Cunff, Licinio Rocha, Vincent Sallet, Corinne Sartel, Alain Lusson, Christophe Couteau, Gilles Lerondel

ZnO nanowires as effective luminescent sensing materials for nitroaromatic derivatives

Roy Aad,*[a] Vesna Simic,[c] Loïc Le Cunff, [a] Licinio Rocha,[c] Vincent Sallet,[b] Corinne Sartel,[b] Alain Lusson,[b] Christophe Couteau[a] and Gilles Lerondel*[a]

We report on the efficient room-temperature photoluminescence (PL) quenching of ZnO in the presence of 2,4-dinitrotoluene (DNT) vapor and for concentration as low as 180 ppb. Compared to ZnO thin films, ZnO nanowires exhibit a strong (95%) and fast (41 s) quenching of the PL intensity in the presence of DNT vapor. Assuming that the PL quenching is due to a trapping of the ZnO excitons by adsorbed DNT molecules, Monte-Carlo calculations show that the nanometric dimensions as well as the better crystallographic quality (longer mean free path) of the ZnO nanowires result in an enhanced trapping process at the origin of the improved sensing properties of the nanowires. The results demonstrate the importance of nanostructures in improving the sensitivity of ZnO. The study also reveals the sensing capability of ZnO nanowires and paves the path towards the potential realization of low-cost sub-ppb nitroaromatic derivative sensors.

Introduction

Selective ultra-trace detection of gas analytes is a central challenge in the field of sensors. Current research aims at not only improving the performances of existing devices[1] (reducing sensitivity threshold, improving selectivity) but also to propose new technological solutions to be able to answer to new needs. For instance, in the case of explosive detection, there are a number of equipments that have proved their worth (e.g. ion mobility spectrometry, mass spectrometry and gas chromatography) but remain rather bulky, expensive and require timeconsuming procedures. Because of these limitations, research focuses on the development of miniaturized sensors that are sufficiently sensitive, selective, inexpensive and compatible with mass production and wide deployment. In this context, nanostructured metal oxide semiconductors are subject to intense studies for sensing applications.[2–4] In particular, zinc oxide (ZnO) nanostructures have been extensively investigated as active materials for toxic gas detection.[5] Due to their particular geometrical (high surface-to-volume ratio) and physical properties, significant improvements in sensor performances (higher sensitivity and faster response time) have been already observed.

The transducing methods that are generally used to detect the presence of chemical vapours consist of monitoring the changes in the electric or piezoelectric properties of ZnO.[6] Moreover, optical based systems which involve coupling with the m-line and the surface plasmon resonance were also addressed and investigated.[7,8] However, the direct impact of gases on ZnO luminescence has never been considered and studied, until recently.[9] This last approach is one of the most promising due to its inherently very high sensitivity and miniaturization capability, as demonstrated for several polymer sensors.[10–12] The reported results on the luminescence quenching of ZnO nanostructures in the presence of volatile organic compounds exhibited ppm level detection,[13–15] which proved the potential of this approach for sensing applications and boosted the motivations towards further nanostructuring challenges and experimental investigations. Some examples have been already reported with systems involving polymeric materials coated onto optically passive nanostructures.[16,17] While ZnO may not be inherently selective compared to polymers, the use of ZnO nanostructure arrays bearing different functional groups influencing the adsorption process may offer a solution to this problem.[18] ZnO also possesses other advantages since it is less prone to photodegradation that might compromise long-term stability and durability, unlike polymers.[19]

In this article, we report on the photoluminescence (PL) quenching of ZnO thin films and nanowires in the presence of 2,4-dinitrotoluene (DNT) vapour. The PL quenching of ZnO in the presence of nitroaromatic derivatives has never been reported yet. Compared to the ZnO thin layer, ZnO nanowires are found to exhibit a fast response time and high quenching efficiency when exposed to DNT. This behaviour can be attributed to the higher surface-to-volume ratio, which characterizes the ZnO nanowire geometry. DNT is a predominant vapour signature found in military grade TNT.[20] Thus, ZnO nanowires are investigated as luminescent sensitive structures for subppm TNT detection.

Experiment

The PL quenching of two ZnO geometries is investigated. The first geometry consists of a 170 nm thick ZnO film (S0), while the second is formed of ZnO nanowires (S1). The thin film and nanowire samples are epitaxially grown by metal–organic chemical vapor deposition in a horizontal reactor operating at a reduced pressure of 65 mbar on R- and A-sapphire substrates respectively. The substrate holder (graphite covered with SiC) can be heated up to 1000 °C using RF induction. Diethylzinc (DEZn) and nitrous oxide (N2O) were respectively used as zinc and oxygen sources, while helium was used as carrier gas. The ZnO thin film is grown at a temperature of 950 °C using a high oxygen/zinc molar ratio of above 14 000, in order to favor a 2D growth and smooth surface morphology. On the other hand, the ZnO nanostructures, consisting of ZnO nanowires emerging on the top of hexagonal pyramids,[21] were grown at a temperature of 875 °C using an oxygen/zinc molar ratio of 940, in order to ensure the formation of vertically aligned nanowires with high aspect ratio.

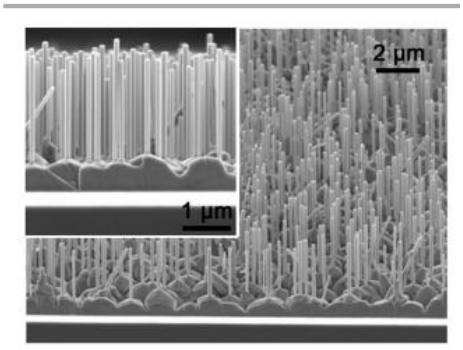

Fig. 1 SEM images of ZnO nanowires deposited on A-sapphire by MOCVD.

Results and discussion

Fig. 1 presents a SEM image of the studied ZnO nanowires. The S1 sample displays vertically aligned nanowires (oriented along the c-axis) with a mean diameter of 130 nm and an average length of 3 µm. The smooth edges of the nanowires clearly evidence their single crystal structure. The high aspect ratio of the S1 structures is hoped to enhance the quenching response of the ZnO material. Fig. 1 also reveals

the presence of a ZnO wetting layer that is inherently formed during the growth of the ZnO nanowires, as already reported.[21–23] Note that such kind of epitaxially grown nanowires can be also obtained on silicon.[24]

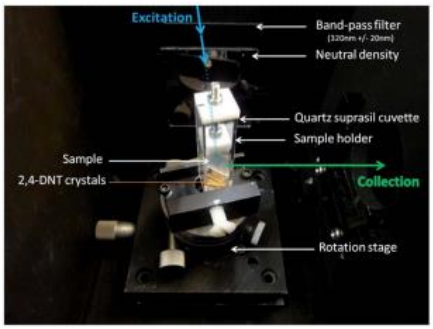

Fig. 2 Picture of the experimental setup used for luminescence quenching studies under static conditions.

Fig. 2 shows an image of the experimental setup that was used to investigate the PL response of the two ZnO samples. As seen in Fig. 2, the ZnO samples are first inserted into a quartz Suprasil cell containing DNT crystals purchased from Fluka (analytical grade standard). The quartz cells containing DNT crystals are prepared one day before the measurements in order to ensure that the DNT concentration has reached equilibrium vapor concentration. At room temperature, the DNT crystals produce a vapor pressure of 160 * 10^{-3} Pa, corresponding to an equilibrium vapor concentration of 180 ppb inside the quartz cell.[25] After insertion, the PL spectrum of the two samples is measured at various time delays using a fluorospectrometer equipped with a 450W xenon lamp. The samples are inserted at the same height as the xenon lamp such as the excitation beam is only exciting the sample and not hitting the DNT crystals. Luminescence spectra are recorded from a wavelength of 350 nm to 600 nm, while the excitation wavelength is set to 335 nm. A bandpass filter around 335 nm is placed in front of the xenon lamp aperture to ensure a monochromatic excitation of the ZnO samples.

Fig. 3 shows the evolution over time of the PL spectrum of the two studied samples in the presence of DNT vapor (left graphs). The PL spectra presented in Fig. 3(a) and (b) are each normalized by the corresponding highest PL intensity at the maximum emission wavelength (λ^{max}_{em}). As seen in Fig. 3, the two samples exhibit similar luminescence peaks with a λ^{max}_{em} at 383 nm, which is attributed to ZnO near-band-edge emission. Most importantly, Fig. 3 reveals a decrease of the PL intensity of the S0 and S1 luminescence due to their exposure to DNT vapor. The PL quenching of ZnO can be attributed to the adsorption of the nitrogen dioxide (NO2) functions existing in the DNT molecules. NO2 molecules are known to adsorb to the ZnO surface through several possible adsorption processes, which involve the trapping of ZnO electrons.[26,27] The electron trapping thus decreases the number of the ZnO charge-carriers (e.g. excitons) that can radiatively recombine. As a consequence, the NO2 adsorption process on the ZnO surface induces a quenching of the ZnO PL intensity. The quenching process is certainly strongly related to the diffusion length of the photo-generated charge-carriers in ZnO and their ability to reach the ZnO surface. While the two samples exhibit PL quenching, they do not present a similar PL quenching efficiency. The ZnO thin film (S0) spectrum presented in Fig. 3(a) displays a very weak, but nonetheless visible, luminescence quenching. On the other hand, in the case of the ZnO nanowires (S1), a remarkably strong and fast decrease of the PL intensity is observed. To quantify the quenching response, the evolution of the lmax em intensity of S0 and S1 as a function of time t is respectively plotted in the right of Fig. 3(a) and (b). The decrease of the λ^{max}_{em} intensity is fitted using exponential decay equations in order to determine the various quenching parameters. The experimental procedure did not allow the measurement of the PL spectrum and subsequently the λ^{max}_{em} intensity, at t = 0 s. Therefore, the experimental data (black circles) were normalized by the extrapolated value of the λ^{max}_{em} intensity at t = 0 s, in order to have the λ^{max}_{em} intensity at t =0 equal to 1. Concerning the ZnO thin film (S0), the PL quenching response is well described by a first-order exponential decay, as shown by the fit (red line) in Fig. 3(a). The fit parameters of the exponential decay (cf. Table 1) deduce a half-time (s) of 290 seconds and a quenching efficiency of 15% for S0. On the other hand, the nanowire (S1) quenching response could not be correctly fitted with a first-order but a second-order exponential decay. The latter speculates two distinct PL quenching processes. The fitting parameters (cf. Table 1) reveal a first (fast) process with a half-time (τ1) of 41 seconds and a second (slow) process with a half-time (τ2) of 414 seconds. The two quenching processes can be explained by the presence of the ZnO nanowires and a ZnO wetting layer in the S1 structure (as seen in Fig. 1). S1 effectively presents a fast response time of the order of τ1, since the fast quenching process constitutes 85% of the overall PL intensity. In addition to the fast response, S1 exhibited a very efficient quenching as 95% of the overall luminescence is quenched. Eventually, while the ZnO thin film response is deficient for TNT detection, nanowires already appear highly suitable for the realization of a low-cost and sub-ppm TNT sensor working at room temperature. The colossal improvement in the quenching response observed between S0 and S1 strongly suggests a geometrical effect. As already mentioned, the luminescence quenching results from an adsorption process of DNT molecules onto the ZnO surface. Thus, the quenching is directly related to the probability of

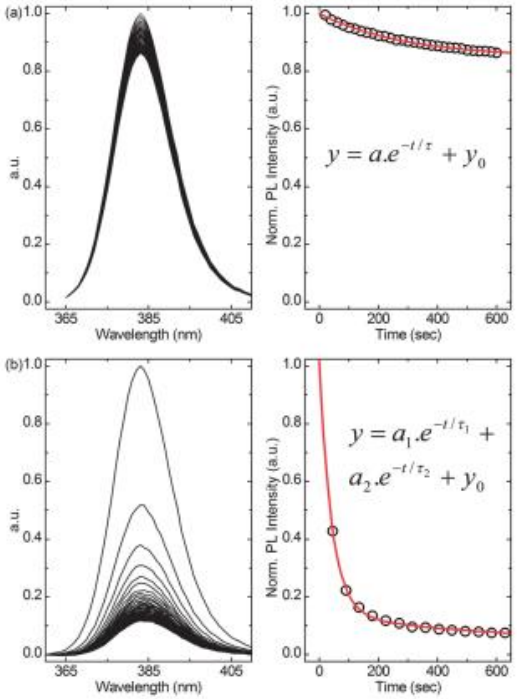

Fig. 3 (a) Evolution of the PL spectrum (to the left) and the λ^{max}_{em} intensity (to the right) of the ZnO thin film (S0) upon exposure to DNT vapor. (b) Evolution of the PL spectrum (to the left) and the λ^{max}_{em} intensity (to the right) of the ZnO nanowires (S1) upon exposure to DNT vapor.

Table 1 Fitting parameters of the exponential decays

	S0	S1	
Equation	$y = ae^{-t/\tau} + y_0$	$y = a_1e^{-t/\tau_1} + a_2e^{-t/\tau_2} + y_0$	
Fit parameters	$\tau = 290$	$\tau_1 = 41$	$\tau_2 = 414$
	$a = 0.15$	$a_1 = 0.85$	$a_2 = 0.1$
	$y_0 = 0.85$	$y_0 = 0.05$	

photo-generated charge-carriers to diffuse and reach the surface in order for them to be trapped. Effectively, in the case of S0, the weak quenching response is somehow expected, since such bulky materials logically present low probabilities for a charge-carrier to reach the contact surface. The increase of the surface-to-volume ratio in the case of nanostructures ensures a large contact area between the DNT and the nanowires and a limited nanowire volume (i.e. stronger charge-carrier spatial confinement) that should ensure an improved probability for charge-carriers to reach the ZnO surface. Therefore, ZnO nanostructures, such as S1, should exhibit an enhanced sensitivity to DNT.

Monte-Carlo simulations were realized in order to show the influence of the geometrical factor on the quenching efficiency in the studied ZnO samples. The Monte-Carlo simulations consist in generating a large number of random-walks for ZnO charge-carriers [e.g. Fig. 4(a), left] in order to determine their probability to reach the surface. In addition, the Monte-Carlo simulation accounts for the absorption at 325 nm in the ZnO structures. Therefore, Monte-Carlo simulations were weighted by a charge-carrier distribution which follows the Beer–Lambert law [e.g. Fig. 4(a), right]. Elastic collisions were considered here. Two parameters are accounted for in the simulations, the mean free path (l) and the diffusion length (L).

Under moderate pumping densities, the photo-generated charge-carriers in ZnO exist as excitons. At room temperature, free excitons usually dominate considering the binding energies.[28] Fig. 4 presents the results obtained by the Monte-Carlo simulation for the thin film (b) and the nanowires (c). The figures show the evolution of the probability for carriers to reach the surface as a function of L and for various values of l. As seen in Fig. 4, the increase of L, as well as the increase of l, increases the probability for the exciton to reach the surface, for both the thin film and the nanowires. Nonetheless, the Monte-Carlo simulation clearly shows the influence of the geometry on the quenching efficiency. As shown in Fig. 4, the nanowires always exhibit a higher probability for excitons to reach the surface than the thin film. In addition, the calculated probability for the thin film [Fig. 4(b)] shows a gradual increase with L and l. For the highest value of L and l (i.e. L = 2000 nm and l = 100 nm), the probability for excitons to reach the thin film surface is however less than 100%. On the other hand, the calculated probability for the nanowires [Fig. 4(c)] shows a strong and sharp increase with the diffusion length and the mean free path. The probability for the excitons to reach the nanowire surface is nearly 100% for L = 1000 nm and l = 20 nm. The experimentally observed quenching efficiencies for the thin film (15%) and the nanowires (95%) can be interpreted with various values of the diffusion length and the mean free path. However the diffusion length (L) of free excitons in ZnO thin films is reported to be between 100 and 200 nm at low temperatures.[29–31] Recent experimental studies have also showed that free excitons of ZnO nanowires possess diffusion lengths around 150 to 200 nm, although measured at low temperatures (5–8 K).[32,33] The diffusion length of free excitons is a parameter mainly related to the nature of the material itself (i.e. ZnO), which explains the similar diffusion lengths observed in thin films and nanowires. However, the mean free path is mostly related to defects in the material and therefore the growth quality. Considering a similar diffusion length of 200 nm for the ZnO, the quenching efficiency of the thin film (i.e. 15%) and the nanowires (i.e. 95%) can be respectively explained by a mean free path of ~ 5 nm and ~ 100 nm, as shown in Fig. 4. The relatively low mean free path in the case of the thin film can be explained by a higher stacking fault density for an epitaxial thin film grown on the R-sapphire substrate as compared with the sample grown on A-sapphire.[34]

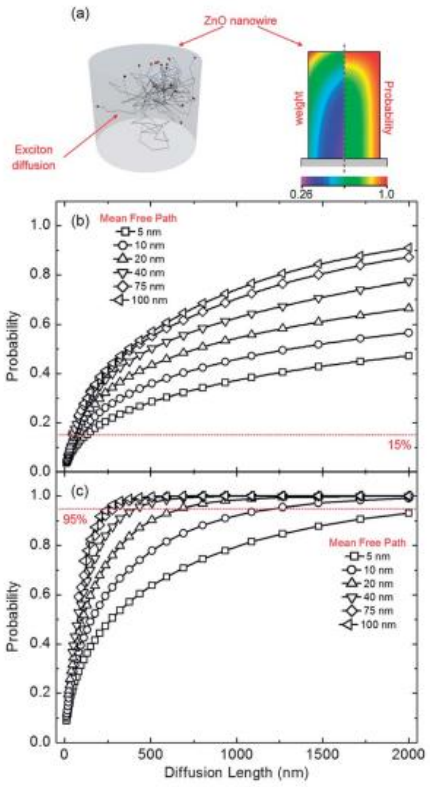

Fig. 4 (a) A 3D representation of a random exciton diffusion path and a cartography of the exciton weight (left side) and probability distribution (right side) at the apex of the nanowire (for symmetry reason only half of the nanowire is represented for each cartography). (b) Probability of exciton reaching the surface of a 170 nm thin film as a function of L for various values of ℓ. (c) Probability of exciton reaching the surface of nanowires of 130 nm diameter and 2 µm height as a function of L for various values of ℓ.

The developed model clearly reveals the important impact of the ZnO geometry, as well as the crystallographic quality (mean free path), on the probability for electrons to reach the ZnO/air interface. However, further experimental investigations will be necessary in order to determine the diffusion lengths of excitons in ZnO at room temperature. Another aspect lies in the DNT concentration at the interface. While it is usually admitted that the quenching efficiency is limited by the probability of the photo-generated carriers to reach the surface, it can also be limited in the case of ultralow concentrations by the density of adsorbed DNT on the ZnO surface. For that respect, the nanometric dimension, as well as the high surface-to-volume ratio, of the nanowires offer better conditions for DNT adsorption.

Conclusion

To conclude, a quenching phenomenon was observed for ZnO thin films and ZnO nanowires in the presence of DNT vapor. The ZnO thin film is characterized by a slow response time (290 s) and a low quenching efficiency (15%). On the other hand, ZnO nanowires exhibited improved quenching properties with a fast response time (41 s) and a high quenching efficiency (95%). The colossal improvement in the ZnO quenching response is attributed to the geometry of the nanowires, which allows for a better trapping of electrons by DNT. This attribution was further confirmed by Monte-Carlo calculations taking into account the diffusion length and the mean free path of the excitons in the materials. This study clearly demonstrates once more the importance of inorganic luminescent nanostructured materials for sensing applications and paves the path towards the realization of efficient low-cost sub-ppm TNT detectors.

Acknowledgements

This work has been supported by the French National Agency (ANR) in the frame of its Programme BLANC (ANR-08-BLAN0296, ULTRAFLU project) and the Champagne-Ardenne Regional council.

Notes and references

1 J. S. Caygill, F. Davis and S. P. J. Higson, Talanta, 2012, 88, 14.

2 D. Spitzer, T. Cottineau, N. Piazzon, S. Josset, F. Schnell, S. N. Pronkin, E. R. Savinova and V. Keller, Angew. Chem., Int. Ed., 2012, 51, 5334.

3 G. S. Aluri, A. Motayed, A. V. Davydov, V. P. Oleshko, K. A. Bertness, N. A. Sanford and M. V. Rao, Nanotechnology, 2011, 22, 295503.

4 A. Yildirim, H. Acar, T. S. Erkal, M. Bayindir and M. O. Guler, ACS Appl. Mater. Interfaces, 2011, 3, 4159.

5 A. Wei, L. Pan and W. Huang, Mater. Sci. Eng., B, 2011, 176, 1409.

6 M. Penza, P. Aversa, G. Cassano, W. Wlodarski and K. Kalantar-Zadeh, Sens. Actuators, B, 2007, 127, 168.

7 T. Mazingue, L. Escoubas, L. Spalluto, F. Flory, P. Jacquouton, A. Perrone, E. Kaminska, A. Piotrowska, I. Mihailescu and P. Atanasov, Appl Opt., 2006, 45, 1425.

8 W.-Y. Feng, N.-F. Chiu, H.-H. Lu, H.-C. Shih, D. Yang and C.-W. Lin, 30th Annual International IEEE EMBS Conference, 2008, p. 5757.

9 D. Valerinia, A. Cretı, A. P. Caricato, M. Lomascolo, R. Rella and M. Martino, Sens. Actuators, B, 2010, 145, 167.

10 J.-S. Yang and T. M. Swager, J. Am. Chem. Soc., 1998, 120, 5321.

11 J. Li, C. E. Kending and E. E. Nesterov, J. Am. Chem. Soc., 2007, 129, 15911.

12 H. Sohn, M. J. Sailor, D. Magde and W. C. Trogler, J. Am. Chem. Soc., 2003, 125, 3821.

13 D. Valerini, A. Cretı, A. P. Caricato, M. Lomascolo, R. Rella and M. Martino, Sens. Actuators, B, 2010, 145, 167.

14 C. Baratto, S. Todros, G. Faglia, E. Comini, G. Sberveglieri, S. Lettieri, L. Santamaria and P. Maddalena, Sens. Actuators, B, 2009, 140, 461.

15 M. C. Carotta, A. Cervi, V. di Natale, S. Gherardi, A. Giberti, V. Guidi, D. Puzzovio, B. Vendemiati, G. Martinelli, M. Sacerdoti, D. Calestani, A. Zappettini, M. Zha and L. Zanotti, Sens. Actuators, B, 2009, 137, 164.

16 A. Rose, Z. Zhu, C. F. Madigan, T. M. Swager and V. Bulovic, Nature, 2005, 434, 876.

17 D. Zhu, Q. He, H. Cao, J. Cheng, S. Feng, Y. Xu and T. Lin, Appl. Phys. Lett., 2008, 93, 261909.

18 X. Fang, L. Hu, C. Ye and L. Zhang, Pure. Appl. Chem., 2010, 82, 2185.

19 F. W. D. Rost, Photobleaching, photoactivation, and quenching in Quantitative Fluorescence Microscopy, Cambridge University Press, New York, 1991, pp. 115–127.

20 V. George, T. F. Jenkins, D. C. Leggett, J. H. Cragin, J. Phelan, J. Oxley and J. Pennington, Proc. SPIE, 1999, 3710, 258.

21 G. Perillat-Merceroz, R. Thierry, P.-H. Jouneau, P. Ferret and G. Feuillet, Nanotechnology, 2012, 23, 125702.

22 W. I. Park, D. H. Kim, S.-W. Jung and G.-C. Yi, Appl. Phys. Lett., 2002, 80, 4232.

23 D. J. Park, J. Y. Lee, D. C. Kim, S. K. Mohanta and H. K. Cho, Appl. Phys. Lett., 2007, 91, 143115.

24 V. Khranovskyy, I. Tsiaoussis, L. Hultman and R. Yakimova, Nanotechnology, 2011, 22, 185603.

25 C. Lenchitz and R. W. Velicky, J. Chem. Eng. Data, 1970, 15, 401.

26 A. Bismuto, S. Lettieri, P. Maddalena, C. Baratto, E. Comini, G. Faglia, G. Sberveglieri and L. Zanotti, J. Opt. A: Pure Appl. Opt., 2006, 8, S585.

27 J. A. Rodriguez, T. Jirsak, J. Dvorak, S. Sambasivan and D. Fischer, J. Phys. Chem. B, 2000, 104, 319.

28 B. K. Meyer, H. Alves, D. M. Hofmann, W. Kriegseis, D. Forster, F. Bertram, J. Christen, A. Hoffmann, M. Straßburg, M. Dworzak, U. Haboeck and A. V. Rodina, Phys. Status Solidi B, 2004, 241, 231.

29 G. Tobin, E. McGlynn, M. O. Henry and J.-P. Mosnier, Appl. Phys. Lett., 2006, 88, 071919.

30 M. Addou, J. Ebothé, A. El Hichou, A. Bougrine, J. L. Bubendorff, M. Troyon, Z. Sofiani, M. EL Jouad, K. Bahedi and M. Lamrani, Cathodoluminescence Properties of Zno Thin Films, Cathodoluminescence, ed. N. Yamamoto, 2012.

31 Z.-M. Liao, H.-C. Wu, Q. Fu, X. Fu, X. Zhu, J. Xu, I. V. Shvets, Z. Zhang, W. Guo, Y. Leprince-Wang, Q. Zhao, X. Wu and D.-P. Yu, Sci. Rep., 2012, 2, 452.

32 J.-S. Hwang, F. Donatini, J. Pernot, R. Thierry, P. Ferret and L. S. Dang, Nanotechnology, 2011, 22, 475704.

33 J. Yoo, B. Chon, W. Tang, T. Joo, L. S. Dang and G.-C. Yi, Appl. Phys. Lett., 2012, 100, 223103.

34 Unpublished results.